Dalton Transactions

ROYAL SOCIETY OF CHEMISTRY

PAPER

View Article Online
View Journal | View Issue

Cite this: *Dalton Trans.*, 2021, **50**, 2472

Synthesis and reactivity of iridium complexes of a macrocyclic PNP pincer ligand†

Thomas M. Hood and Adrian B. Chaplin *

Received 18th December 2020,
Accepted 19th January 2021

DOI: 10.1039/d0dt04303f

rsc.li/dalton

Having recently reported on the synthesis and rhodium complexes of the novel macrocyclic pincer ligand PNP-14, which is derived from lutidine and features terminal phosphine donors *trans*-substituted with a tetradecamethylene linker (*Dalton Trans.*, 2020, **49**, 2077–2086 and *Dalton Trans.*, 2020, **49**, 16649–16652), we herein describe our findings critically examining the chemistry of iridium homologues. The five-coordinate iridium(I) and iridium(III) complexes [Ir(PNP-14)(η^2:η^2-cyclooctadiene)][BAr^F_4] and [Ir(PNP-14)(2,2′-biphenyl)][BAr^F_4] are readily prepared and shown to be effective precursors for the generation of iridium(III) dihydride dihydrogen, iridium(I) bis(ethylene), and iridium(I) carbonyl derivatives that highlight important periodic trends by comparison to rhodium counterparts. Reaction of [Ir(PNP-14)$H_2(H_2)$][BAr^F_4] with 3,3-dimethylbutene induced triple C–H bond activation of the methylene chain, yielding an iridium(III) allyl hydride derivative [Ir(PNP-14*)H][BAr^F_4], whilst catalytic homocoupling of 3,3-dimethylbutyne into *Z*-*t*BuC≡CCHCH*t*Bu could be promoted at RT by [Ir(PNP-14)(η^2:η^2-cyclooctadiene)][BAr^F_4] ($TOF_{initial}$ = 28 h^{-1}). The mechanism of the latter is proposed to involve formation and direct reaction of a vinylidene derivative with HC≡C*t*Bu outside of the macrocyclic ring and this suggestion is supported experimentally by isolation and crystallographic characterisation of a catalyst deactivation product.

1. Introduction

Phosphine-based pincers are robust ancillary ligands that continue to find notable applications in organometallic chemistry and homogenous catalysis.[1,2] In particular, rhodium and iridium complexes of these ligands are associated with fundamental and applied breakthroughs in the chemistry of C–H bond activation reactions; exemplified by the characterisation of σ-alkane complexes and development of high-performance alkane dehydrogenation catalysts, respectively.[3,4] These *mer*-tridentate ligands are evidently well-suited to supporting the formation of highly reactive M(I) derivatives necessary to bring about cleavage of strong C–H bonds,[5] able to accommodate the changes in geometry associated with M(I)/M(III) redox shuttling, and suitably modular in composition to enable augmentation of metal-based reactivity through considered change of the central donor atom, wingtip substituents, or backbone constituents.[2] As marked out by lower carbonyl stretching frequencies,[6] the heavier iridium congeners are particularly notable for a more pronounced tendency for oxidative addition of H_2,[7,8] C(sp^3)–H bonds,[3,9] and C(sp^2)–H bonds[10] compared to their rhodium counterparts.

Motivated by the potential to exploit additional reaction control though their unique steric profile, use in the construction of interlocked assemblies, and as an extension of our related work with NHC-based variants,[11–13] we have recently become interested in the chemistry of macrocyclic phosphine-based pincers.[14–16] Last year we reported on the synthesis and rhodium complexes of the lutidine-derived macrocyclic pincer PNP-14, where the chiral P-donors are *trans*-substituted with a tetradecamethylene linker (Chart 1).[14,15] As a novel platform for exploring the organometallic chemistry of Group 9 pincer complexes, we now present our findings critically examining

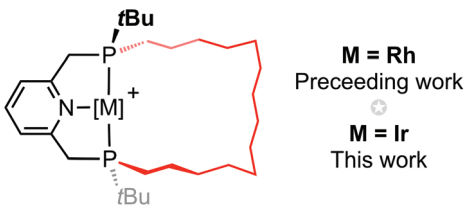

Chart 1 Complexes of the macrocyclic pincer ligand PNP-14.

Department of Chemistry, University of Warwick, Gibbet Hill Road, Coventry CV4 7AL, UK. E-mail: a.b.chaplin@warwick.ac.uk

†Electronic supplementary information (ESI) available: Catalytic homocoupling of 3,3-dimethylbutyne promoted by **6**, synthesis and characterisation of [Rh(PNP-14)(η^2-norbornene)][BAr^F_4]; NMR, IR and ESI-MS spectra of new compounds, and selected reactions (PDF). Primary NMR data (MNOVA). CCDC 2051203–2051207. For ESI and crystallographic data in CIF or other electronic format see DOI: 10.1039/d0dt04303f

the chemistry of iridium PNP-14 homologues aided by reference to acyclic complexes of 2,6-$(R_2PCH_2)_2C_5H_3N$ (PNP-R; *e.g.* R = *t*Bu, *i*Pr).

2. Results and discussion

Mirroring synthetic strategies that we have successfully employed for rhodium homologues,[14,15] the preparation of iridium(I) and iridium(III) complexes of PNP-14 was attempted through substitution reactions of $[Ir(COD)_2][BAr^F_4]$[17] in 1,2-difluorobenzene (DFB) and $[Ir(COD)(biph)Cl]_2$ [18] in fluorobenzene, respectively, with the latter exploiting $Na[BAr^F_4]$ as a halide abstracting agent (COD = 1,5-cyclooctadiene, Ar^F = 3,5-$(CF_3)_2C_6H_3$, biph = 2,2′-biphenyl; Scheme 1). These reactions produced five-coordinate cationic derivatives $[Ir(PNP\text{-}14)(\eta^2{:}\eta^2\text{-}COD)][BAr^F_4]$ **1** and $[Ir(PNP\text{-}14)(biph)][BAr^F_4]$ **2** under mild conditions, which were subsequently isolated as analytically pure crystalline materials in good yield (*ca.* 80%) and fully characterised (Scheme 1).

Iridium(I) complex **1** adopts a distorted trigonal bipyramidal metal geometry (18 VE), with the terminal phosphine donors positioned in the equatorial coordination sites conferring a distinctly puckered pincer ligand geometry. Distortion of the PNP ligand towards a *fac* coordination mode in this manner is associated with a compressed P–Ir–P bite angle of 115.24(2)° in the solid state and a pair of ^{31}P resonances at δ 17.0 and 13.4 with no appreciable $^2J_{PP}$ coupling in DFB solution. While unusual, the formulation of **1** simply appears to be a consequence of COD chelation, although this is contingent upon the flexible lutidine-based backbone and asymmetric steric profile of the phosphine donors.[19] Moreover, given the rhodium(I) homologue is instead characterised as a C_1-symmetric square planar complex, *viz.* $[Rh(PNP\text{-}14)(\eta^2\text{-}COD)]^+$(**1′**, 16 VE; δ_{31P} 57.4, 45.9, $^2J_{PP}$ = 312 Hz),[15,20] the capacity of the heavier metal congener to from stronger metal–ligand bonds is clearly a decisive factor. Bulk purity was established by combustion analysis and the structure of **1** was fully corroborated in solution by NMR spectroscopy and HR ESI-MS.

Coordination of PNP-14 is more conventional in the formally 16 VE square pyramidal iridium(III) complex **2**, as evidenced by a P–Ir–P bite angle of 163.24(5)° in the solid state and C_1 symmetry in CD_2Cl_2 solution; with a pair of ^{31}P resonances at δ 38.7 and 20.9 exhibiting a characteristically large *trans*-phosphine $^2J_{PP}$ coupling constant of 307 Hz.[21] The crystal structure of **2** is isomorphous to the direct rhodium homologue **2′**,[14] with the tetradecamethylene linker skewed to one side of the basal plane away from the biph ligand and contorted in such a way as to enable adoption of a weak γ-agostic interaction (**2**, Ir1···H–C129 = 3.152(7); *cf.* 3.184(2) Å for **2′**). Previously reported five-coordinate complexes of the form $[M(pincer)(biph)][BAr^F_4]$ provide further structural precedent for **2** and the metal-based metrics of the acyclic analogue $[Ir(PNP\text{-}tBu)(biph)][BAr^F_4]$ (**II**) are similar.[6,11,14] Moreover, as **II** is fluxional in solution as a result

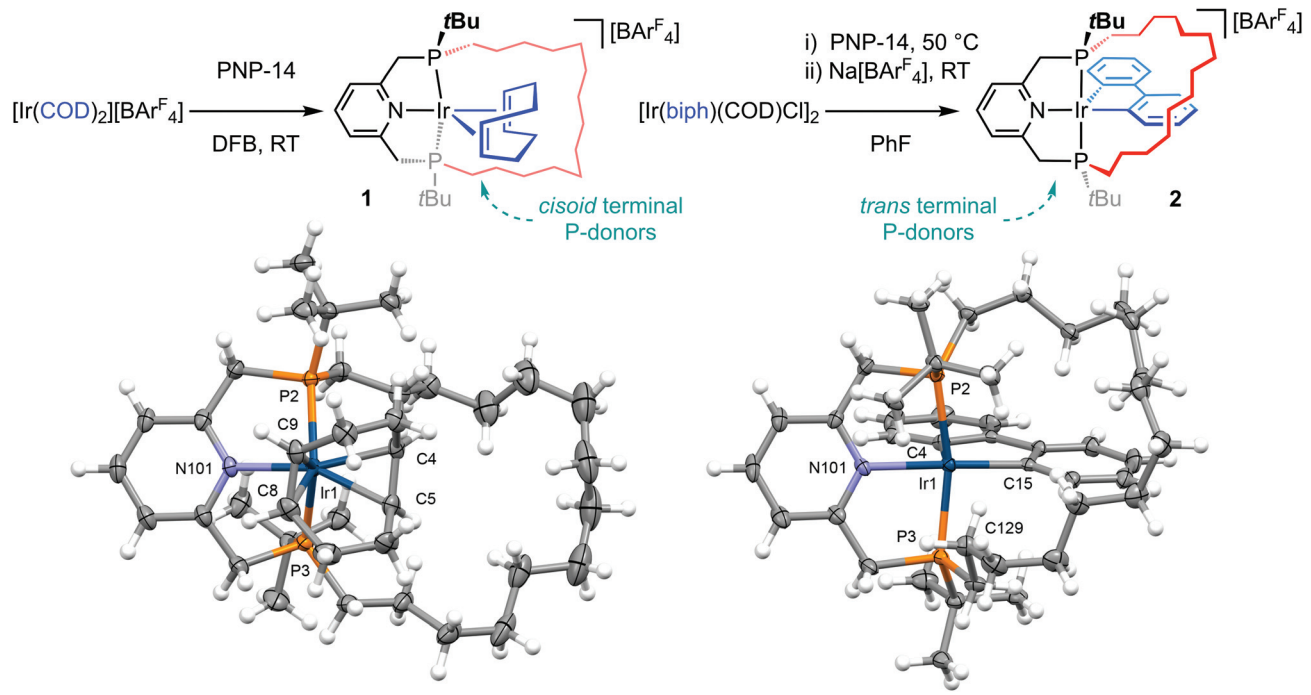

Scheme 1 Synthesis and solid-state structures of iridium pincer complexes **1** and **2**: thermal ellipsoids at 50% and 30% probability, respectively; anions omitted. Selected bond lengths (Å) and angles (°): **1**, Ir1–P2, 2.3743(7); Ir1–P3, 2.3846(7); P2–Ir1–P3, 115.24(2); Ir1–N101, 2.107(2); Ir1–Cnt (C4,C5), 2.083(2); Ir1–Cnt(C8, C9), 2.036(2); N101–Ir1–Cnt(C4, C5), 172.52(8); Cnt(C4, C5)–Ir–Cnt(C8, C9), 84.29(9); **2**, Ir1–P2, 2.3253(15); Ir1–P3, 2.2849(15); P2–Ir1–P3, 163.24(5); Ir1–N101, 2.158(5); Ir1–C4, 2.048(6); Ir1–C15, 2.044(6); N101–Ir1–C15, 172.5(2); C4–Ir1–C15, 81.9(2); Ir1···C129, 3.152(7); Ir1···HC129, 2.54; Cnt = centroid.

of facile biph pseudorotation on the NMR timescale,[6] retention of C_1 symmetry in solution suggests that buttressing with the methylene strap prevents such dynamics in **2**.

Reaction of **2** with dihydrogen (1 atm) in DFB at RT resulted in immediate and full conversion into [Ir(PNP-14)(2-biphenyl)H][BAr^F_4] **3** ($\delta_{^{31}P}$ 40.6, 36.5, $^2J_{PP}$ = 302 Hz; $\delta_{^1H}$ −21.6; Scheme 2). No further reaction was observed after 18 h, but heating at 85 °C for 6 h resulted in complete hydrogenolysis of the biph ligand and formation of dihydride dihydrogen complex [Ir(PNP-14)$H_2(H_2)$][BAr^F_4] **4** in quantitative spectroscopic yield. Hydrogenolysis also occurs for **2′** and **II**, but longer reaction times are required under otherwise equivalent conditions (both *ca.* 2 days).[14] Coordinatively saturated **1** rapidly affords **4** upon reaction with dihydrogen (1 atm) in DFB at RT (<5 min), invoking facile and reversible chelation of COD.

Complex **4** was characterised *in situ* using NMR spectroscopy, with adoption of time-averaged C_2 symmetry, a single ^{31}P resonance at δ 42.1, and a broad 4H resonance at δ −9.26 (T_1 = 88.8 ± 0.7 ms, 600 MHz, argon) the most diagnostic features at 298 K. The hydride signal remained broad upon cooling to 253 K but exhibits faster spin–lattice relaxation (δ −9.27, T_1 = 50 ± 1 ms, 600 MHz, argon). The acyclic analogue [Ir(PNP-*t*Bu)$H_2(H_2)$][BF_4] (**IV**) is known and formulation as a dihydride dihydrogen complex was corroborated in a similar manner *in situ* by NMR spectroscopy.[7] Whilst the data was recorded under difference conditions, the similarly of the hydride signatures is striking (**IV**, $\delta_{^1H}$ −9.31, T_1 = 24 ms, 400 MHz, 233 K in CD_3OD). In line with the reduced propensity for oxidative addition, the rhodium homologue of **4** is instead observed as a dihydrogen complex, *viz.* [Rh(PNP-14)(H_2)][BAr^F_4] **4′**.[14]

Further supporting the assignment of **4**, reaction with ethylene (1 atm) generated the corresponding C_1-symmetric dihydride π-complex **5** ($\delta_{^{31}P}$ 33.4, 12.4, $^2J_{PP}$ = 314; $\delta_{^1H}$ −7.89, −17.80) within 5 min at RT (Scheme 2). Subsequent heating at 85 °C for 16 h yielded the bis(ethylene) complex **6** ($\delta_{^{31}P}$ 9.0) in quantitative spectroscopic yield, with concomitant formation of ethane. C_2 symmetry and coordination of two molecules of ethylene was established *in situ* by NMR spectroscopy. The latter is associated with four chemically inequivalent 2H signals at δ 3.23, 2.80, 2.49 and 1.97 and two ^{13}C resonances at δ 26.0 and 18.0, and reinforces the disposition of iridium(I) centres to adopt five-coordinate geometries: as seen in **2**, but contrasting that observed under the same conditions in the rhodium(I) system, *viz.* [Rh(PNP-14)(C_2H_4)][BAr^F_4] **6′**.[14] Structurally-related bis(ethylene) iridium(I) complexes of CNC- and pybox-based pincer ligands have been crystallographically characterised, exhibiting distorted trigonal bipyramidal metal geometries with the ethylene ligands located in the equatorial sites,[22] but are unknown for PNP- and PONOP-based ligands.[23]

When **2** was instead treated with an excess of 3,3-dimethylbutene (5 equivalents) the allyl hydride derivative [Ir(PNP-14*)H][BAr^F_4] **7** was produced in quantitative spectroscopic yield after 5 days heating at 100 °C, presumably through intramolecular transfer dehydrogenation of the methylene chain followed by allylic C–H activation (Scheme 2).[24] As precedent for this reactivity, examples of cyclometallated rhodium(III) and iridium(III) pincer complexes can be found in the literature.[25] Complex **7** was subsequentially isolated in 49% yield and fully characterised, including in the solid state by single crystal X-ray diffraction (Fig. 1). In solution **7** is distinctly C_1-symmetric, with a pair of ^{31}P resonances at δ 81.4 and 25.8 with $^2J_{PP}$ = 313 Hz, allyl ^{13}C resonances at δ 81.9, 66.0, and 38.9, and a 1H hydride resonance at δ −8.49 ($^2J_{PH}$ = 19.6, 9.7 Hz). The crystal structure demonstrates that **7** adopts a pseudo-octahedral metal geometry in the solid state, with κ_6-coordination of PNP-14* creating iridacyclopentyl and iridacyclododecyl rings, and the hydride ligand was located from the Fourier difference map. Little distortion of the PNP-core is evident in **7** and the associated metal-based metrics are broadly comparable to those in **2** (*e.g.* P–Ir–P *ca.* 163°). There is considerable variance in the allyl Ir–C bond lengths, with the longest contact *trans* to the hydride ligand (Ir1–C119 = 2.311(4) Å, Ir1–C120, 2.155(3) Å, Ir1–C121, 2.199(3) Å), but all the internal carbon bond angles are >120°. The geometry of

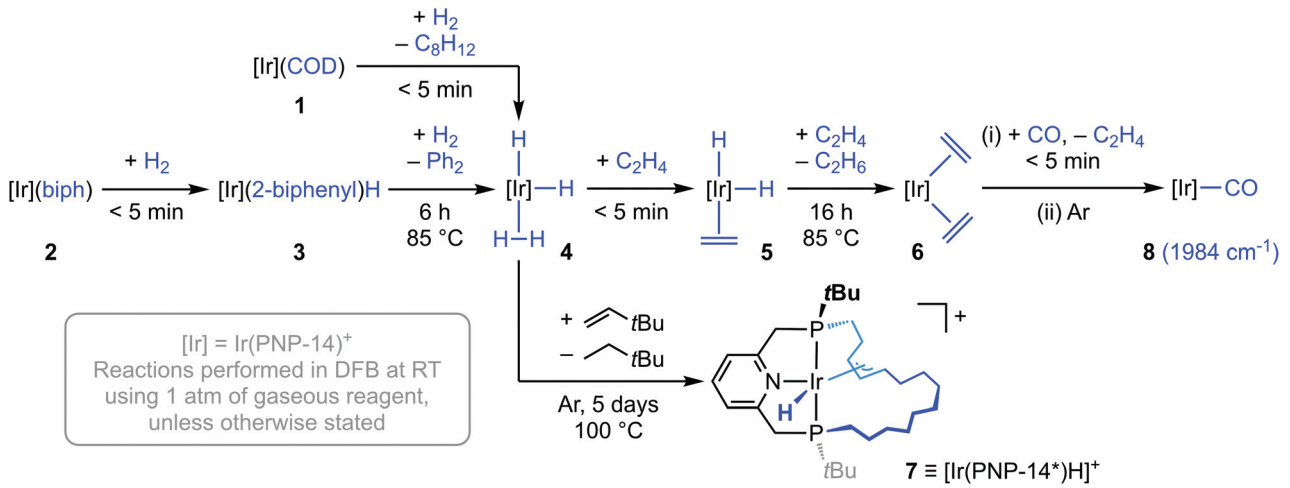

Scheme 2 Synthesis and reactivity of iridium dihydride dihydrogen complex **4**. [BAr^F_4]$^-$ counter anions omitted for clarity.

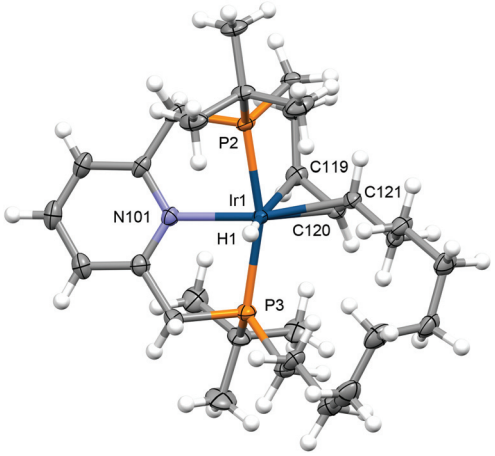

Fig. 1 Solid-state structure of **7**: the hydride ligand was located from the Fourier difference map; thermal ellipsoids at 30% probability; solvent molecule and anion omitted. Selected bond lengths (Å) and angles (°): Ir1–P2, 2.2694(8); Ir1–P3, 2.3339(9); P2–Ir1–P3, 163.04(3); Ir1–N101, 2.126(2); Ir1–H1, 1.39(3); Ir1–C119, 2.311(4); Ir1–C120, 2.155(3); Ir1–C121, 2.199(3); C119–C120, 1.430(5); C120–C121, 1.409(5); C119–C120–C121, 124.4(3); N101–Ir1–C121, 169.59(11).

the iridacyclododecyl ring is reminiscent of the quadrilateral conformations adopted by 12-membered cycloalkanes.[26]

The onward reactivity of **6** was harnessed to access the C_2-symmetric Ir(I) carbonyl derivative **8** ($\delta_{^{31}P}$ 62.5) by reaction with carbon monoxide, which was isolated in 89% yield (overall from **2**; Scheme 2). Complexes of this nature are of interest as the carbonyl ligand is a convenient spectroscopic reporter group for the electronic characteristics of the metal-pincer fragment.[27,28] In this case, the ν(CO) band of **8** (1984 cm^{-1}) is shifted to considerably lower frequency compared to the rhodium(I) homologue **8′** (1997 cm^{-1}) under the same conditions (CH_2Cl_2 solution, Table 1). This is in line with expected periodic trends, which are also apparent from the IR data collected for *t*Bu- and *i*Pr-substituted analogues. These data suggest that PNP-14 is a marginally weaker net donor than PNP-*t*Bu, but equivalent to PNP-*i*Pr.[14]

Of the organometallic chemistry we have discovered so far using PNP-14, the capacity for rhodium complexes to promote the stoichiometric homocoupling of 3,3-dimethylbutyne through the annulus of the macrocyclic ligand stands out (**1′** → **9′** in Scheme 3).[15] Given that a structurally related Ir(PCP) system has also been shown to promote stoichiometric terminal alkyne coupling reactions,[30,31] we were very interested to ascertain if similar reactivity could be brought about in iridium complexes of PNP-14. Iridium(I) complex **1** was selected as the most suitable precursor and initial screening studies using a twofold excess of HC≡C*t*Bu in DFB at RT indicated rapid production of the corresponding *Z*-enyne ($\delta_{^1H}$ 5.53, 5.25; $^3J_{HH}$ = 11.9 Hz)[32] without any observable consumption of **1** (Scheme 3). This stereochemistry contrasts that observed for the rhodium system and, as homocoupling through the macrocycle would be expected to result in an interpenetrated enyne complex, it appears that production of the enyne occurs catalytically outside the ring. Subsequent detailed investigation of this reaction using 100 equivalents HC≡C*t*Bu confirmed that **1** is an effective precatalyst.[33] Under these conditions, the dimerisation of HC≡C*t*Bu into *Z*-*t*BuC≡CCHCH*t*Bu proceeds with an initial TOF of 28 h^{-1}. After 6 h, analysis by ^{1}H NMR spectroscopy indicated complete consumption of HC≡C*t*Bu and exclusive production of *Z*-*t*BuC≡CCHCH*t*Bu. From the $^{31}P\{^1H\}$ NMR spectrum generation of a new organometallic species was apparent (**10**, δ 25.0, 16.3; $^2J_{PP}$ = 364 Hz), accounting for 88% of the metal-containing species with **1** making up 10%. Addition of a further 50 equivalents of HC≡C*t*Bu induced complete conversion of **1** into **10** within 24 h but coincided with a halt in homocoupling, which plateaued at 65 TONs.

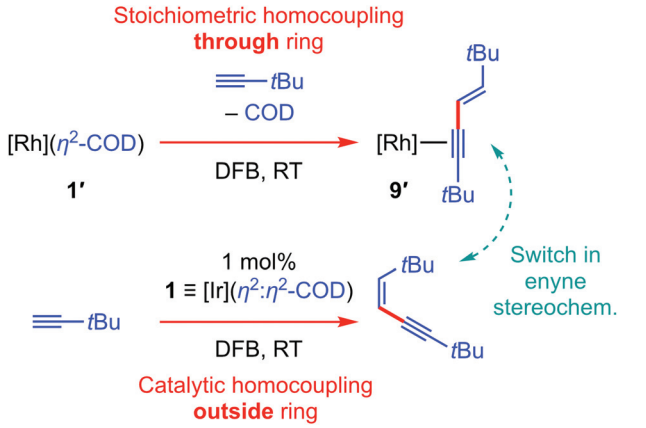

Scheme 3 Terminal alkyne coupling reactions promoted by **1** and **1′**: [M] = M(PNP-14)$^+$.

Repeating the homocoupling reaction on a larger scale under similar conditions enabled isolation of **10** from solution in 76% yield, which was subsequently identified as iridium(III) bis(alkenyl) complex [Ir(PNP-14)(η^3-*E*-C(C≡C*t*Bu)CH*t*Bu)(η^1-*E*-CHCH*t*Bu)][BAr^F_4] (Scheme 4). In the solid state, **10** adopts a very distorted octahedral geometry with the alkenyl ligands in a *cis* configuration (C4–Ir1–C6 = 102.50(9)°) and coordination of the σ-organyl derived from *Z*-*t*BuC≡CCHCH*t*Bu reinforced by π-complexation of the alkyne (Ir1–alkyne = 2.505(2) Å): a binding mode, for which there are no crystallographically characterised Group 9 precedents to our knowledge (CSD 5.41).[34] The respective alkenyl Ir–C and C=C bond lengths are not statistically different (Ir1–C4 = 2.043(2) Å, Ir1–C6 = 2.053(2) Å; C4–C5 = 1.330(3) Å, C6–C9 = 1.329(3) Å). The structure of **10**

Table 1 Carbonyl stretching frequencies (CH_2Cl_2)

Pincer	ν(CO)/cm^{-1}	Ref.
[Ir(PNP-14)(CO)][BAr^F_4] **8**	1984	This work
[Rh(PNP-14)(CO)][BAr^F_4] **8′**	1997	14
[Ir(PNP-*t*Bu)(CO)][BAr^F_4]	1977	6
[Rh(PNP-*t*Bu)(CO)][BAr^F_4]	1990	6
[Ir(PNP-*i*Pr)(CO)][BAr^F_4]	1986[a]	29
[Rh(PNP-*i*Pr)(CO)][BAr^F_4]	1998	27

[a] Measured in the solid state (ATR).

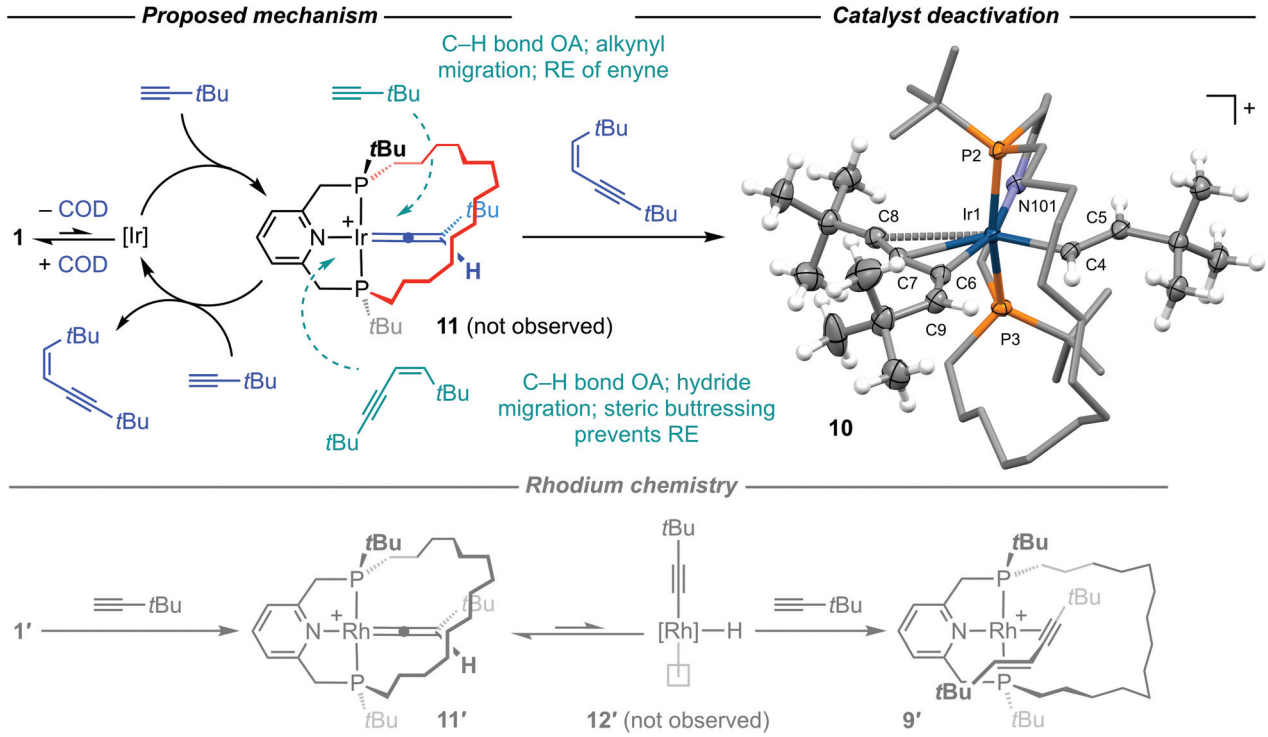

Scheme 4 Mechanistic features of the terminal alkyne coupling reactions promoted by **1** and **1′**: [M] = M(PNP-14)$^+$ and [BAr$^F_4$]$^-$ counter anions omitted. Solid-state structure of **10** depicted with thermal ellipsoids at 30% probability for selected atoms; minor disordered component (IrP$_2$ core), most H atoms, and anion omitted; structural diagram provided in the experimental section. Selected bond lengths (Å) and angles (°): Ir1–P2, 2.3141 (5); Ir1–P3, 2.3659(5); P2–Ir1–P3, 163.55(2); Ir1–N101, 2.122(2); Ir–C4, 2.043(2); Ir–C4–C5, 129.59(15); C4–C5, 1.330(3); Ir1–C6, 2.053(2); Ir1–C6–C9, 147.4(2); C6–C9, 1.329(3); Ir1–Cnt(C7, C8), 2.505(2); C6–C7–C8, 161.9(2); C7–C8, 1.216(3); N101–Ir1–C6, 159.35(8); C4–Ir1–Cnt(C7, C8), 153.16 (7); C4–Ir1–C6, 102.50(9); Cnt = centroid.

determined by X-ray crystallography was fully corroborated in solution using NMR spectroscopy. For instance, the alkenyl ^{1}H resonances are located at δ 7.81 (IrC<u>H</u>C*t*Bu; $^3J_{HH}$ = 15.0 Hz), 5.68 (IrCC<u>H</u>*t*Bu), and 4.78 (IrCHC<u>H</u>*t*Bu; $^3J_{HH}$ = 15.2 Hz) in a 1 : 1 : 1 ratio, with the associated ^{13}C resonances at δ 143.5 (IrCH<u>C</u>H*t*Bu), 142.2 (IrC<u>C</u>H*t*Bu), 105.3 (Ir<u>C</u>CH*t*Bu), and 95.7 (Ir<u>C</u>HCH*t*Bu); the α-carbons exhibiting coupling to ^{31}P ($^2J_{PC}$ = 5–10 Hz). The HR-ESI MS of **10** is also notable for a strong $[M]^+$ ion signal at 916.5623 (calcd 916.5628) *m*/*z* and bulk purity of was confirmed by combustion analysis.

Terminal alkyne homocoupling reactions that produce *Z*-enyne products are generally understood to proceed *via* vinylidene intermediates, with **11** implicated in this case (Scheme 4).[35,36] Indeed, the rhodium homologue **11′** is produced initially upon reaction of **1′** with HC≡C*t*Bu.[15] Reaction with the second alkyne equivalent, by net 1,2-addition of the constituent C(sp)–H bond across the vinylidene M=C linkage (concerted or step-wise) followed by reductive elimination, would thereafter confer the enyne product. *E*-Enyne isomers such as that observed in the rhodium system can also be produced in this manner, although an indirect route involving equilibrium generation of the rhodium(III) alkynyl hydride **12′** is instead invoked in the formation of **9′** from **11′** (Scheme 4). Whilst **11** was not detected during the formation of *Z*-*t*BuC≡CCHC*t*Bu, the generation of **10** provides strong circumstantial evidence for its intermediate presence. No reaction between **1** and independently synthesised *Z*-*t*BuC≡CCHCH*t*Bu in DFB was observed, even upon heating at 50 °C for 1 h. The formation of the bis(alkenyl) is, therefore, most reasonably reconciled by irreversible reaction of *Z*-*t*BuC≡CCHCH*t*Bu with **11**; involving net 1,2-addition of the {C≡C}C(sp^2)–H bond across the Ir=C linkage. The addition evidently takes place through the ring in this instance, with the macrocycle preventing subsequent reductive elimination.[12] We therefore attribute the generation of **10** to catalyst deactivation by irreversible product inhibition. The postulated reactivity of the Group 9 vinylidenes derived from **1** and **1′** is clearly nuanced by the nature of the metal and impact of the unique steric constraints imposed by the tetradecamethylene linker. We believe that the more facile Ir(I)/Ir(III) redox couple and propensity of the {Ir(PNP-14)}$^+$ fragment to adopt geometries with the pincer ligand in a non-meridional conformation are the decisive factors. Specifically, we propose that the *Z*-selective homocoupling of HC≡C*t*Bu proceeds catalytically outside the ring *via* C(sp)–H bond oxidative addition of HC≡C*t*Bu to **11** affording *fac*-[Ir(PNP-14)(CCH*t*Bu)(C≡C*t*Bu)H]$^+$, alkynyl migration yielding an enynyl hydride, and finally release of *Z*-*t*BuC≡CCHCH*t*Bu by reductive elimination. In contrast, **1′** mediates the stoichiometric *E*-selective homocoupling of HC≡C*t*Bu through the ring ultimately *via* a pathway bypassing the vinylidene intermediate **11′**. Further computational analysis would be required to corroborate these sug-

gestions, although accurately modelling the effect of the methylene chain is non-trivial.

3. Conclusions

The organometallic chemistry of iridium complexes of the macrocyclic PNP-14 pincer ligand has been explored. The five-coordinate iridium(I) and iridium(III) complexes [Ir(PNP-14)(η^2:η^2-COD)][BAr^F_4] **1** and [Ir(PNP-14)(biph)][BAr^F_4] **2** are readily prepared and fully characterised derivatives, with the former notable for a distorted trigonal bipyramidal metal geometry in which the pincer ligand adopts an unusual non-meridional confirmation, and the latter for adoption of a square pyramidal metal geometry stabilised by a weak γ-agostic interaction between the metal and the tetradecamethylene linker. These well-defined complexes have been shown to be effective precursors for the generation of iridium(III) dihydride dihydrogen (**4**), iridium(I) bis(ethylene) (**6**), and iridium(I) carbonyl (**8**) derivatives that highlight important periodic trends by comparison to rhodium counterparts: *i.e.* the more facile oxidative addition of dihydrogen, propensity to from five-coordinate d^8 complexes, and greater π-basicity of the heavier metal conger, respectively.

Onward reactivity of the {Ir(PNP-14)}$^+$ fragment was also explored with the bulky unsaturated substrates 3,3-dimethylbutene and 3,3-dimethylbutyne. Reaction of **4** with 3,3-dimethylbutene induced triple C–H bond activation of the methylene chain yielding an iridium(III) allyl hydride complex [Ir(PNP-14*)H][BAr^F_4] **7**, whilst **1** is an effective pre-catalyst for the homocoupling of 3,3-dimethylbutyne into *Z*-*t*BuC≡CCHCH*t*Bu under mild conditions. The latter is particularly remarkable given that reaction of the homologous rhodium precursor **1′** results in the formation of an interpenetrated *E*-enyne complex (**9′**). The mechanism of the homocoupling promoted by **1** is proposed to involve formation and direct reaction of the (unobserved) vinylidene derivative [Ir(PNP-14)(CCH*t*Bu)][BAr^F_4] (**11**) with HC≡C*t*Bu outside of the macrocyclic ring. This suggestion is supported experimentally by isolation and crystallographic characterisation of [Ir(PNP-14)(η^3-*E*-C(C≡C*t*Bu)CH*t*Bu)(η^1-*E*-CHCH*t*Bu)][BAr^F_4] (**10**), which results from deactivation of the catalyst by product inhibition.

4. Experimental

4.1 General methods

All manipulations were performed under an atmosphere of argon using Schlenk and glove box techniques unless otherwise stated. Dihydrogen and ethylene were dried by passage through a column of activated 3 Å molecular sieves. Glassware was oven dried at 150 °C overnight and flame-dried under vacuum prior to use. Molecular sieves were activated by heating at 300 °C *in vacuo* overnight. Fluorobenzene and DFB were pre-dried over Al_2O_3, distilled from calcium hydride and dried twice over 3 Å molecular sieves.[37] CD_2Cl_2 was freeze–pump–thaw degassed and dried over 3 Å molecular sieves. C_6D_6 was distilled from sodium and stored over 3 Å molecular sieves. $SiMe_4$ was distilled from liquid Na/K alloy and stored over a potassium mirror. Other anhydrous solvents and liquid reagents were purchased from Acros Organics or Sigma-Aldrich, freeze–pump–thaw degassed and stored over 3 Å molecular sieves. PNP-14,[14] [Ir(COD)$_2$][BAr^F_4],[17] [Ir(biph)(COD)Cl]$_2$,[18] Na[BAr^F_4],[38] and [Ir(PNP-*t*Bu)(biph)][BAr^F_4] (**II**)[6] were synthesized according to published procedures. All other solid reagents are commercial products and were used as received. NMR spectra were recorded on Bruker spectrometers under argon at 298 K unless otherwise stated. Chemical shifts are quoted in ppm and coupling constants in Hz. Virtual coupling constants are reported as the separation between the first and third lines. NMR spectra in DFB were recorded using an internal capillary of C_6D_6 or acetone-d_6.[37] High resolution ESI-MS were recorded on Bruker Maxis Plus instrument. Infrared spectra were recorded on a Jasco FT-IR-4700 using a KBr transmission cell in CH_2Cl_2. Microanalyses were performed at the London Metropolitan University by Stephen Boyer or Elemental Microanalysis Ltd.

4.2 Preparation of [Ir(PNP-14)(η^2:η^2-COD)][BAr^F_4] (1)

A solution of [Ir(COD)$_2$][BAr^F_4] (29.3 mg, 23.0 μmol) and PNP-14 (11.0 mg, 23.0 μmol) in DFB (0.5 mL) was mixed for 5 min at RT, the volatiles were removed *in vacuo* and the resulting orange oil washed with pentane (2 × 2 mL). The analytically pure product was obtained as a yellow crystalline solid by slow diffusion of $SiMe_4$ (*ca.* 10 mL) into a DFB solution (0.5 mL) at −30 °C. Yield: 29.0 mg (17.7 μmol, 77%).

^{1}H NMR (500 MHz, DFB): δ 8.11–8.16 (m, 8H, Ar^F), 7.50 (br, 4H, Ar^F), 7.33 (t, $^3J_{HH}$ = 7.7, 1H, py), 7.08 (d, $^3J_{HH}$ = 7.7, 1H, py), 7.03 (obscured, py), 4.25–4.34 (m, 1H, Ir(CH=CH){axial}), 4.34–4.44 (m, 1H, Ir(CH=CH){axial}), 3.72 (d, $^2J_{PH}$ = 6.6, 2H, pyC$\underline{H}_2$), 3.51 (dd, $^2J_{HH}$ = 18.2, $^2J_{PH}$ = 6.0, 1H, pyC$\underline{H}_2$), 3.34 (dd, $^2J_{HH}$ = 18.2, $^2J_{PH}$ = 9.7, 1H, pyC$\underline{H}_2$), 2.54–2.66 (m, 2H, CH_2), 2.15–2.45 (m, 6H, CH_2 + 1 × Ir(CH=CH){equatorial} [δ 2.39]), 1.38–2.04 (m, 9H, CH_2 + 1 × Ir(CH=CH){equatorial} [δ 1.83]), 1.38 (d, $^3J_{PH}$ = 12.7, 9H, *t*Bu), 0.94–1.32 (m, 19H, CH_2), 0.65 (d, $^3J_{PH}$ = 12.5, 9H, *t*Bu).

^{13}C{^{1}H} NMR (126 MHz, DFB): δ 163.7 (dd, J_{PC} = 5, 4, py), 162.5 (q, $^1J_{CB}$ = 50, Ar^F), 162.4 (obscured, py), 138.2 (s, py), 135.1 (s, Ar^F), 129.7 (qq, $^2J_{FC}$ = 32, $^3J_{CB}$ = 3, Ar^F), 124.9 (q, $^1J_{FC}$ = 272, Ar^F), 122.0 (d, $^3J_{PC}$ = 6, py), 120.7 (d, $^3J_{PC}$ = 8, py), 117.6 (sept, $^3J_{FC}$ = 4, Ar^F), 64.7 (br, Ir(CH=CH){axial}), 60.9 (d, $^2J_{PC}$ = 3, Ir(CH=CH){axial}), 60.2 (dd, $^2J_{PC}$ = 27, 4, Ir(CH=CH){equatorial}), 50.1 (dd, $^2J_{PC}$ = 29, $^2J_{PC}$ = 5, Ir(CH=CH){equatorial}), 45.6 (dd, $^1J_{PC}$ = 27, $^3J_{PC}$ = 4, py$\underline{C}H_2$) 42.3 (d, $^1J_{PC}$ = 22, py$\underline{C}H_2$), 35.8 (d, $^3J_{PC}$ = 10, CH_2), 35.5 (br, CH_2), 35.2 (dd, $^1J_{PC}$ = 19, $^3J_{PC}$ = 4, *t*Bu{C}), 34.1 (d, $^1J_{PC}$ = 7, PCH_2), 33.4 (br, *t*Bu{C}), 31.1 (d, $^3J_{PC}$ = 10, CH_2), 29.8 (d, $^3J_{PC}$ = 9, CH_2), 29.7 (s, CH_2), 29.5 (s, CH_2), 29.3 (d, $^1J_{PC}$ = 17, PCH_2), 29.0 (s, CH_2), 28.8 (s, CH_2), 28.7 (s, CH_2), 28.6 (br, CH_2), 28.3 (s, CH_2), 28.12 (s, CH_2), 28.05 (s, CH_2), 27.8 (d, $^2J_{PC}$ = 4, *t*Bu{CH_3}), 27.1 (d, $^3J_{PC}$ = 7, CH_2), 27.0 (s, CH_2), 26.6 (s, CH_2), 26.4 (d, $^2J_{PC}$ = 5, *t*Bu{CH_3}).

^{31}P{^{1}H} NMR (162 MHz, DFB): δ 17.0 (s, 1P), 13.4 (s, 1P).

HR ESI-MS (positive ion 4 kV): 778.4221 ($[M]^+$, calcd 778.4218) *m*/*z*.

Anal. calcd for $C_{69}H_{77}BF_{24}IrNP_2$ (1641.32 g mol^{-1}): C, 50.49; H, 4.73; N, 0.85. Found: C, 50.40; H, 4.64; N, 0.87.

4.3 NMR scale reaction of 1 with dihydrogen

A solution of **1** (12.2 mg, 7.43 μmol) in DFB (0.5 mL) within a J. Young valve NMR tube was freeze–pump–thaw degassed and placed under an atmosphere of dihydrogen (1 atm). Analysis by NMR spectroscopy indicated quantitative formation of **4** with concomitant formation of COD within 5 min at RT.

4.4 Preparation of [Ir(PNP-14)(biph)][BAr$^F_4$] (2)

A suspension of PNP-14 (13.3 mg, 27.8 μmol) and [Ir(biph)(COD)Cl]$_2$ (13.7 mg, 14.0 μmol) in fluorobenzene (0.50 mL) was stirred for 2 days at 50 °C to give a pale-yellow solution. Na[BAr$^F_4$] (24.7 mg, 27.9 μmol) was added and the suspension stirred for a further 4 h at RT. The volatiles were removed *in vacuo* and the resulting purple oil was washed with pentane (2 × 1 mL), dried *in vacuo* and then the product extracted into CH_2Cl_2 (2 mL). The analytically pure product was obtained as a purple crystalline solid by recrystallisation from CH_2Cl_2 : hexane (1 : 20) at −30 °C. Yield: 36.4 mg (21.6 μmol, 78%).

^{1}H NMR (500 MHz, CD_2Cl_2): δ 8.00 (t, $^3J_{HH}$ = 7.9, py, 1H), 7.70–7.76 (m, 10H, py + Ar^F), 7.64 (d, $^3J_{HH}$ = 7.6, 1H, biph), 7.60 (d, $^3J_{HH}$ = 7.5, 1H, biph), 7.56 (br, 4H, Ar^F), 7.39 (d, $^3J_{HH}$ = 7.6, 1H, biph), 7.19 (t, $^3J_{HH}$ = 7.3, 1H, biph), 7.10 (t, $^3J_{HH}$ = 7.5, 1H, biph), 6.88 (t, $^3J_{HH}$ = 7.4, 1H, biph), 6.33 (t, $^3J_{HH}$ = 7.8, 1H, biph), 5.35 (d, $^3J_{HH}$ = 8.2, 1H, biph), 4.02 (dd, $^2J_{HH}$ = 19.4, $^2J_{PH}$ = 9.6, 1H, pyCH$_2$), 3.75–3.89 (m, 2H, 2 × pyCH$_2$), 3.50 (dd, $^3J_{HH}$ = 17.0, $^3J_{HH}$ = 9.2, 1H, pyCH$_2$), 3.02–3.15 (m, 1H, PCH$_2$), 2.78–2.88 (m, 1H, PCH$_2$), 1.88–1.98 (m, 1H, CH$_2$), 0.66–1.73 (m, 23H, CH$_2$), 1.16 (d, $^3J_{PH}$ = 14.0, 9H, *t*Bu), 0.49 (d, $^3J_{PH}$ = 16.1, 9H, *t*Bu), 0.22–0.37 (m, 2H, CH$_2$).

^{13}C{^{1}H} NMR (126 MHz, CD_2Cl_2): δ 164.6 (app t, J_{PC} = 4, py), 163.3 (br, py), 162.3 (q, $^1J_{CB}$ = 50, Ar^F), 150.6 (d, $^3J_{PC}$ = 2 biph), 149.6 (s, biph), 145.3 (dd, $^2J_{PC}$ = 8, 6, biph{IrC}), 139.9 (s, py), 135.4 (s, Ar^F), 135.2 (s, biph), 129.42 (qq, $^2J_{FC}$ = 32, $^3J_{CB}$ = 3, Ar^F), 129.39 (s, biph), 126.3 (s, biph), 125.6 (s, biph), 125.3 (s, biph), 125.1 (q, $^1J_{FC}$ = 272, Ar^F), 123.5 (s, biph), 123.2 (d, $^3J_{PC}$ = 10, py), 123.1 (d, $^3J_{PC}$ = 9, py), 122.1 (s, biph), 121.3 (s, biph), 121.2 (app t, $^2J_{PC}$ = 6, biph{IrC}), 118.0 (sept, $^3J_{FC}$ = 4, Ar^F), 40.9 (d, $^1J_{PC}$ = 29, pyCH$_2$), 39.5 (d, $^1J_{PC}$ = 26, pyCH$_2$), 35.0 (d, $^1J_{PC}$ = 23, *t*Bu{C}), 32.9 (d, $^2J_{PC}$ = 14, CH$_2$), 32.8 (obscured, *t*Bu{C}), 30.4 (s, CH$_2$), 29.6 (s, CH$_2$), 29.5 (s, CH$_2$), 29.42 (s, CH$_2$), 29.35 (s, CH$_2$), 29.2 (s, CH$_2$), 29.1 (d, $^2J_{PC}$ = 3, *t*Bu{CH$_3$}), 28.1 (s, CH$_2$), 27.9 (d, $^1J_{PC}$ = 28, PCH$_2$), 27.3 (s, CH$_2$), 25.8 (br, CH$_2$), 25.5 (s, *t*Bu{CH$_3$}), 24.7 (s, CH$_2$), 24.1 (s, CH$_2$), 19.7 (dd, $^1J_{PC}$ = 22, $^3J_{PC}$ = 3, PCH$_2$).

^{31}P{^{1}H} NMR (162 MHz, CD_2Cl_2): δ 38.7 (d, $^2J_{PP}$ = 307, 1P), 20.9 (d, $^2J_{PP}$ = 307, 1P).

HR ESI-MS (positive ion, 4 kV): 822.3912 ($[M]^+$, calcd 822.3906) *m*/*z*.

Anal. calcd for $C_{73}H_{73}BF_{24}IrNP_2$ (1685.33 g mol^{-1}): C, 52.03; H, 4.37; N, 0.83; found: C, 51.88; H, 4.28; N, 0.81.

4.5 NMR scale reactions of 2

The following reactions were carried out starting with a solution of **2** (16.9 mg, 10.0 μmol) in DFB (0.5 mL) within a J. Young valve NMR tube and analysed *in situ* by NMR spectroscopy.

4.5.1 Synthesis of [Ir(PNP-14)(2-biphenyl)H][BAr$^F_4$] (3). The solution of **2** was freeze–pump–thaw degassed and placed under dihydrogen (1 atm), resulting in quantitative formation of **3** within 5 min at RT. No free biphenyl was observed.

^{1}H NMR (400 MHz, DFB, H_2, selected data): δ 7.61 (t, $^3J_{HH}$ = 7.8, 1H py), 3.66–3.82 (m, 2H, 2 × pyCH$_2$), 3.06 (dd, $^2J_{HH}$ = 17.3, $^2J_{PH}$ = 6.4, 1H, pyCH$_2$), 0.79 (d, $^3J_{PH}$ = 13.4, 9H, *t*Bu), 0.67 (d, $^3J_{PH}$ = 14.1, 9H, *t*Bu), −21.6 (app t, $^2J_{PH}$ = 15, 1H, IrH).

^{31}P{partial ^{1}H} NMR (162 MHz, DFB, H_2): δ 40.6 (dd, $^2J_{PP}$ = 302, $^2J_{PH}$ = 14, 1P), 36.5 (dd, $^2J_{PP}$ = 302, $^2J_{PH}$ = 14, 1P).

4.5.2 Synthesis of [Ir(PNP-14)H$_2$(H$_2$)][BAr$^F_4$] (4). The solution of **3** was heated at 85 °C for 6 h, resulting quantitative formation **4** with concomitant formation of biphenyl ($\delta_{^1H}$ 7.42, 7.25, 7.16).

^{1}H NMR (500 MHz, DFB, H_2): δ 8.10–8.16 (m, 8H, Ar^F), 7.49 (br, 4H, Ar^F), 7.47 (t, $^3J_{HH}$ = 7.8, 1H, py), 7.19 (d, $^3J_{HH}$ = 7.8, 2H, py), 3.96 (dvt, $^2J_{HH}$ = 17.6, J_{PH} = 8, 2H, pyCH$_2$), 3.12 (dvt, $^2J_{HH}$ = 17.6, J_{PH} = 10, 2H, pyCH$_2$), 2.11–2.23 (m, 2H, PCH$_2$), 1.12–1.69 (m, 26H, CH$_2$), 0.91 (vt, J_{PH} = 16, 18H, *t*Bu), −9.27 (br, fwhm = 24 Hz, 4H, IrH$_4$).

^{13}C{^{1}H} NMR (126 MHz, DFB, H_2): δ 162.3 (q, $^1J_{CB}$ = 50, Ar^F), 162.4 (vt, J_{PC} = 6, py), 138.9 (s, py), 135.1 (s, Ar^F), 129.7 (qq, $^2J_{FC}$ = 32, $^3J_{CB}$ = 3, Ar^F), 124.9 (q, $^1J_{FC}$ = 272, Ar^F), 120.4 (vt, J_{PC} = 10, py), 117.6 (sept, $^3J_{FC}$ = 4, Ar^F), 44.4 (vt, J_{PC} = 28, pyCH$_2$), 30.0 (vt, J_{PC} = 32, *t*Bu{C}), 29.0 (s, CH$_2$), 28.9 (vt, J_{PC} = 8, CH$_2$), 28.3 (s, CH$_2$), 28.2 (s, CH$_2$), 27.5 (s, CH$_2$), 26.3 (s, CH$_2$), 25.8 (vt, J_{PC} = 32, PCH$_2$), 24.5 (vt, J_{PC} = 6, *t*Bu{CH$_3$}).

^{31}P{^{1}H} NMR (162 MHz, DFB, H_2,): δ 42.1 (s, 2P).

^{1}H NMR (600 MHz, DFB, Ar, 298 K, selected data): δ −9.26 (br, fwhm = 29 Hz, T_1 = 88.8 ± 0.7 ms, 4H, IrH).

^{1}H NMR (600 MHz, DFB, Ar, 253 K, selected data): δ −9.27 (br, fwhm = 21 Hz, T_1 = 50 ± 1, 4H, IrH).

4.5.3 Synthesis of [Ir(PNP-14)H$_2$(C$_2$H$_4$)][BAr$^F_4$] (5). The solution of **4** was freeze–pump–thaw degassed and placed under ethylene (1 atm), resulting in quantitative formation of **5** within 5 min at RT.

^{1}H NMR (500 MHz, DFB, C_2H_4, selected data): δ 7.43 (t, $^3J_{HH}$ = 7.8, 1H, py), 3.71–3.84 (m, 2H, 2 × pyCH$_2$), 3.18–3.37 (m, 5H, 1 × pyCH$_2$ + 4 × C_2H_4), 3.08 (dd, $^2J_{HH}$ = 17.6, $^2J_{PH}$ = 10.4, 1H, pyCH$_2$), 0.89 (d, $^3J_{PH}$ = 14.9, 9H, *t*Bu), 0.87 (d, $^3J_{PH}$ = 13.9, 9H, *t*Bu), −7.89 (dd, $^2J_{PH}$ = 17.6, $^2J_{PH}$ = 13.1, 1H, IrH), −17.80 (app t, J_{PH} = 11, 1H, IrH).

^{13}C{^{1}H} NMR (126 MHz, DFB, C_2H_4, selected data): δ 48.7 (s, C_2H_4).

^{31}P{^{1}H} NMR (162 MHz, DFB, C_2H_4): δ 33.4 (d, $^2J_{PP}$ = 314, 1P), 12.4 (d, $^2J_{PP}$ = 314, 1P).

4.5.4 Synthesis of [Ir(PNP-14)(C$_2$H$_4$)$_2$][BAr$^F_4$] (6). The solution of **5** was heated at 85 °C for 16 h, resulting in quantitative formation of **6**, with concomitant formation of ethane ($\delta_{^1H}$ 0.70, $\delta_{^{13}C}$ 6.1).

^{1}H NMR (600 MHz, DFB, C_2H_4): δ 8.11–8.15 (m, 8H, $Ar^F{}_4$), 7.50 (br, 4H, $Ar^F{}_4$), 7.46 (t, $^3J_{HH}$ = 7.8, 1H, py), 7.15 (d, $^3J_{HH}$ = 7.8, 2H, py), 3.63 (dvt, $^2J_{HH}$ = 16.8, J_{PH} = 8, 2H, pyC$\underline{H}_2$), 3.28 (dvt, $^2J_{HH}$ = 16.8, J_{PH} = 8, 2H, pyC$\underline{H}_2$), 3.23 (br, 2H, C_2H_4), 2.80 (br, 2H, C_2H_4), 2.49 (br, 2H, C_2H_4), 1.97 (br, 2H, C_2H_4), 1.03–1.48 (m, 28H, CH_2), 0.79 (br, 18H, *t*Bu).

^{13}C{^{1}H} NMR (126 MHz, DFB, C_2H_4): δ 164.1 (d, $^3J_{PC}$ = 3, py), 162.6 (q, $^1J_{CB}$ = 50, Ar^F), 139.1 (s, py), 135.1 (s, Ar^F), 129.7 (qq, $^2J_{FC}$ = 32, $^3J_{CB}$ = 3, Ar^F), 124.9 (q, $^1J_{FC}$ = 272, Ar^F), 119.8 (vt, J_{PC} = 8, py), 117.6 (sept, $^3J_{FC}$ = 4, Ar^F), 42.6 (vt, J_{PC} = 28, py$\underline{C}H_2$), 33.5 (vt, J_{PC} = 26, *t*Bu{C}), 31.0 (s, CH_2), 29.1 (vt, J_{PC} = 12, CH_2), 27.8 (s, CH_2), 27.3 (s, CH_2), 27.2 (s, CH_2), 26.3 (s, *t*Bu{CH_3}), 26.0 (s, C_2H_4), 24.6 (s, CH_2), 18.0 (s, C_2H_4), 14.3 (vt, J_{PC} = 24, PCH_2).

^{31}P{^{1}H} NMR (162 MHz, DFB, C_2H_4): δ 9.0 (s, 2P).

4.5.5 Synthesis and isolation of [Ir(PNP-14)(CO)][$BAr^F{}_4$] (8). The solution of **6** was freeze–pump–thaw degassed and placed under carbon monoxide (1 atm), resulting in an immediate colour change from colourless to bright yellow. The volatiles were removed *in vacuo*, and the resulting yellow oil washed with $SiMe_4$ (2 × 0.5 mL) and thoroughly dried *in vacuo* to give the analytically pure product as a yellow foam. Yield: 13.9 mg (8.90 μmol, 89%).

^{1}H NMR (500 MHz, CD_2Cl_2): δ 7.87 (t, $^3J_{HH}$ = 7.8, 1H, py), 7.70–7.76 (m, 8H, Ar^F), 7.56 (br, 4H, Ar^F), 7.51 (d, $^3J_{HH}$ = 7.9, 2H, py), 3.94 (dvt, $^2J_{HH}$ = 17.6, J_{PH} = 8, 2H, pyC$\underline{H}_2$), 3.47 (dvt, $^2J_{HH}$ = 17.6, J_{PH} = 8, 2H, pyC$\underline{H}_2$), 2.18–2.27 (m, 4H, PCH_2), 1.94–2.07 (m, 2H, CH_2), 1.76–1.89 (m, 2H, CH_2), 1.64–1.74 (m, 2H, CH_2), 1.54–1.64 (m, 2H, CH_2), 1.23–1.48 (m, 16H, CH_2), 1.14 (vt, J_{PH} = 16, 18H, *t*Bu)

^{13}C{^{1}H} NMR (126 MHz, CD_2Cl_2): δ 182.5 (vt, $^2J_{PC}$ = 18, CO), 165.4 (vt, J_{PC} = 10, py), 162.3 (q, $^1J_{CB}$ = 50, Ar^F), 141.9 (s, py), 135.4 (s, Ar^F), 129.4 (qq, $^2J_{FC}$ = 32, $^3J_{CB}$ = 3, Ar^F), 125.2 (q, $^1J_{FC}$ = 272, Ar^F), 122.0 (vt, J_{PC} = 10, py), 118.0 (sept, $^3J_{FC}$ = 4, Ar^F), 39.4 (vt, J_{PC} = 24, py$\underline{C}H_2$), 34.7 (vt, J_{PC} = 30, *t*Bu{C}), 30.3 (vt, J_{PC} = 10 CH_2), 29.3 (s, CH_2), 29.0 (s, CH_2), 28.9 (s, CH_2), 28.3 (s, CH_2), 27.5 (vt, J_{PC} = 6, *t*Bu{CH_3}), 26.1 (s, CH_2), 23.4 (vt, J_{PC} = 30, PCH_2).

^{31}P{^{1}H} NMR (162 MHz, CD_2Cl_2): δ 64.6 (s, 2P).

^{31}P{^{1}H} NMR (162 MHz, DFB): δ 62.5 (s, 2P).

IR (CH_2Cl_2): ν(CO) 1984 cm^{-1}.

HR ESI-MS (positive ion, 4 kV): 698.3217 ([*M*]$^+$, calcd 698.3228) *m*/*z*.

Anal. calcd for $C_{62}H_{65}BF_{24}IrNOP_2$ (1561.14 g mol^{-1}): C, 47.70; H, 4.20; N, 0.90; found: C, 47.89; H, 4.13; N, 0.97.

4.6 NMR scale reaction of [Ir(PNP-*t*Bu)(biph)][$BAr^F{}_4$] (II) with dihydrogen

A solution of **II** (16.0 mg, 9.98 μmol) in DFB (0.5 mL) within a J. Young valve NMR tube was freeze–pump–thaw degassed and placed under dihydrogen (1 atm) and then heated at 80 °C for 2 days. Analysis by NMR spectroscopy indicated quantitative formation of [Ir(PNP-*t*Bu)$H_2(H_2)$][$BAr^F{}_4$]. The spectroscopic data are consistent with the literature for the related BF_4^- salt.[7]

^{1}H NMR (400 MHz, CD_2Cl_2, selected data): δ 8.11–8.17 (m, 8H, Ar^F), 7.50 (s, 4H, Ar^F), 3.52 (vt, J_{PH} = 8, 4H, pyC$\underline{H}_2$), 1.11 (vt, J_{PH} = 14, 36H, *t*Bu), −9.48 (br, 4H, IrH).

^{31}P{^{1}H} NMR (162 MHz, DFB): δ 64.6 (s, 2P).

4.7 Preparation of [Ir(PNP-14*)H][$BAr^F{}_4$] (7)

A solution of **4** (13.6 μmol, generated *in situ* as described above) in DFB (0.5 mL) within a J. Young valve NMR tube was treated with 3,3-dimethylbutene (8.8 μL, 71.4 μmol) and the solution heated at 100 °C for 5 days. Analysis by NMR spectroscopy indicated quantitative formation of the product. The volatiles were removed *in vacuo* and the resulting pink/red oil washed with $SiMe_4$ (2 × 0.5 mL). The analytically pure product was obtained as pale red blocks by the slow diffusion of excess $SiMe_4$ into a DFB solution at −30 °C. Yield: 10.2 mg (6.66 μmol, 49%).

^{1}H NMR (500 MHz, CD_2Cl_2): δ 7.70–7.75 (m, 8H, Ar^F), 7.65 (t, $^3J_{HH}$ = 7.8, 1H, py), 7.56 (br, 4H, Ar^F), 7.34 (d, $^3J_{HH}$ = 7.8, 1H, py), 7.31 (d, $^3J_{HH}$ = 7.8, 1H, py), 4.86 (app q, J_{HH} = 9, 1H, IrCH), 4.47 (app t, $^3J_{HH}$ = 7, 1H, IrCH), 3.71–3.81 (m, 2H, 2 × pyC$\underline{H}_2$), 3.41 (dd, $^2J_{HH}$ = 17.1, $^2J_{PH}$ = 9.3, 1H, pyC$\underline{H}_2$), 3.26 (dd, $^2J_{HH}$ = 17.4, $^2J_{PH}$ = 9.2, 1H, pyC$\underline{H}_2$), 2.35–2.52 (m, 1H, CH_2), 2.15–2.29 (m, 1H, CH_2), 1.98–2.11 (m, 1H, CH_2), 0.94–1.95 (m, 20H, IrCH [δ 1.89] + CH_2), 1.17 (d, $^3J_{PH}$ = 15.4, 9H, *t*Bu), 1.01 (d, $^3J_{PH}$ = 13.5, 9H, *t*Bu), −8.49 (dd, $^2J_{PH}$ = 19.6, 9.7, 1H, IrH).

^{13}C{^{1}H} NMR (126 MHz, CD_2Cl_2): δ 163.4 (br, py), 162.3 (q, $^1J_{CB}$ = 50, Ar^F), 161.9 (br, py), 138.5 (s, py), 135.4 (s, Ar^F), 129.4 (qq, $^2J_{FC}$ = 32, $^3J_{CB}$ = 3, Ar^F), 125.1 (q, $^1J_{FC}$ = 272, Ar^F), 121.0 (d, $^3J_{PC}$ = 9, py), 120.8 (d, $^3J_{PC}$ = 9, py), 118.0 (sept, $^3J_{FC}$ = 4, Ar^F), 81.9 (s, IrCH), 66.0 (d, $^2J_{PC}$ = 5, IrCH), 41.9 (d, $^1J_{PC}$ = 30, py$\underline{C}H_2$), 39.2 (d, $^1J_{PC}$ = 29, py$\underline{C}H_2$), 38.9 (s, IrCH), 35.9 (s, CH_2), 35.0 (dd, $^1J_{PC}$ = 22, $^3J_{PC}$ = 5, *t*Bu{C}), 30.4 (dd, $^1J_{PC}$ = 22, $^3J_{PC}$ = 5, *t*Bu{C}), 29.6 (s, CH_2), 27.8 (d, $^2J_{PC}$ = 14, CH_2), 27.4 (s, CH_2), 27.0 (d, $^2J_{PC}$ = 3, *t*Bu{CH_3}), 25.7 (d, $^2J_{PC}$ = 4, *t*Bu{CH_3}), 24.8 (dd, $^1J_{PC}$ = 28, $^3J_{PC}$ = 1, PCH_2), 24.4 (s, CH_2), 24.3 (d, $^2J_{PC}$ = 5, CH_2), 22.9 (s, CH_2), 22.3 (s, CH_2), 21.6 (s, CH_2), 20.8 (dd, $^1J_{PC}$ = 24, $^3J_{PC}$ = 4, PCH_2).

^{31}P{^{1}H} NMR (162 MHz, CD_2Cl_2): δ 81.4 (d, $^2J_{PP}$ = 313, 1P), 25.8 (d, $^2J_{PP}$ = 313, 1P).

^{31}P{^{1}H} NMR (162 MHz, DFB): δ 80.9 (d, $^2J_{PP}$ = 313, 1P), 25.5 (d, $^2J_{PP}$ = 313, 1P).

HR ESI-MS (positive ion 4 kV): 668.3128 ([*M*]$^+$, calcd 668.3122) *m*/*z*.

Anal. calcd for $C_{62}H_{67}BF_{24}IrNP_2$ (1531.12 g mol^{-1}): C, 47.85; H, 4.15; N, 0.91. Found: C, 47.65; H, 4.03; N, 1.01.

4.8 NMR scale reaction of 7 with dihydrogen

A solution of **7** (7.7 mg, 5.03 μmol) in DFB (0.5 mL) within a J Young valve NMR tube was freeze–pump–thaw degassed, placed under dihydrogen (1 atm) and heated at 80 °C for 16 h. Analysis by NMR spectroscopy indicated quantitative formation of **4**.

4.9 Catalytic homocoupling of 3,3-dimethylbutyne promoted by 1

A solution of **1** (8.2 mg, 5.0 μmol) in DFB (400 μL) within a J. Young NMR tube was treated with a solution of 3,3-dimethylbutyne (62 μL, 503 μmol) and the resulting homocoupling

reaction producing only *Z*-*t*BuC≡CCHCH*t*Bu followed at RT *in situ* using NMR spectroscopy. The solution was mixed constantly when not in the spectrometer. Analysis after 1 hour indicated 28 TONs, with complete conversion observed within 6 h. At this point, **10** was observed as the major organometallic species (88%), with **1** the minor organometallic species (10%). Further 3,3-dimethylbutyne (31 μL, 252 μmol) was added, resulting in further homocoupling, totalling 65 TONs and complete conversion of **1** to **10** after 24 h. Spectroscopic data for *Z*-*t*BuC≡CCHCH*t*Bu is consistent with literature values.[32]

Data for *Z*-*t*BuC≡CCHCH*t*Bu:**^{1}H NMR** (400 MHz, DFB, selected data): δ 5.53 (d, $^3J_{HH}$ = 11.9, 1H, CH═CH), 5.25 (d, $^3J_{HH}$ = 11.9, 1H, CH═CH), 1.12 (s, 9H, *t*Bu), 1.11 (s, 9H, *t*Bu).

4.10 Preparation of [Ir(PNP-14)(η^3-*E*-C(C≡C*t*Bu)CH*t*Bu)(η^1-*E*-CHCH*t*Bu)][BAr$^F{}_4$] (10)

A solution of **1** (14.0 mg, 8.53 μmol) in DFB (0.5 mL) within a J Young valve NMR tube was treated with 3,3-dimethylbutyne (210 μL, 1.71 mmol) and stirred for 6 h at RT. Analysis by NMR spectroscopy indicated quantitative formation of the product. The volatiles were removed *in vacuo*, the resulting yellow oil washed with $SiMe_4$ (2 × 0.5 mL) and dried *in vacuo* to afford the analytically product as a yellow solid. Yield: 11.6 mg (6.52 μmol, 76%). Crystals suitable X-ray crystallography were obtained by slow diffusion of excess $SiMe_4$ into an Et_2O solution. From the $SiMe_4$ washings *Z*-*t*BuC≡CCHCH*t*Bu was obtained as a colourless oil in low yield. Yield: 4.6 mg (28.0 μmol, 2%).

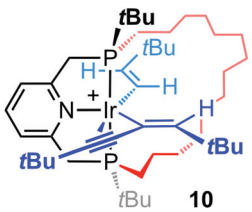

10

^{1}H NMR (500 MHz, CD_2Cl_2): δ 7.83 (t, $^3J_{HH}$ = 6.7, 1H, py), 7.81 (dd, $^3J_{HH}$ = 15.0, $^3J_{PH}$ = 3, 1H, IrCHCH*t*Bu), 7.70–7.75 (m, 8H, Ar^F), 7.56 (br, 4H, Ar^F), 7.52 (d, $^3J_{HH}$ = 7.9, 1H, py), 7.49 (d, $^3J_{HH}$ = 7.9, 1H, py), 5.68 (t, $^4J_{PC}$ = 2, 1H, IrCCH*t*Bu), 4.78 (dt, $^3J_{HH}$ = 15.2, $^4J_{PH}$ = 2, 1H, IrCHCH*t*Bu), 4.28 (ddd, $^2J_{HH}$ = 16.5, $^2J_{PH}$ = 10.3, $^4J_{PH}$ = 3.0, 1H, pyCH$_2$), 3.69 (ddd, $^2J_{HH}$ = 17.4, $^2J_{PH}$ = 10.1, $^4J_{PH}$ = 1.3, 1H, pyCH$_2$), 3.64 (dd, $^2J_{HH}$ = 17.4, $^2J_{PH}$ = 9.9, 1H, pyCH$_2$), 3.22 (dd, $^2J_{HH}$ = 16.5, $^2J_{PH}$ = 7.9, 1H, pyCH$_2$), 2.28–2.43 (m, 2H, CH$_2$), 2.08–2.19 (m, 1H, CH$_2$), 0.88–1.96 (m, 25H, CH$_2$), 1.24 (s, 9H, IrCCH*t*Bu), 1.17 (s, 9H, C≡C*t*Bu),1.02 (d, $^3J_{PH}$ = 14, 18H, 2 × P*t*Bu), 1.00 (s, 9H, IrCHCH*t*Bu).

^{13}C{^{1}H} NMR (126 MHz, CD_2Cl_2): δ 164.2 (app t, J_{PC} = 3, py), 163.3 (app t, J_{PC} = 3, py), 162.3 (q, $^1J_{CB}$ = 50, Ar^F), 143.5 (app t, $^3J_{PC}$ = 4, IrCHCH*t*Bu), 142.2 (br, IrCCH*t*Bu), 139.4 (s, py), 135.4 (s, Ar^F), 129.4 (qq, $^2J_{FC}$ = 32, $^3J_{CB}$ = 3, Ar^F), 125.1 (q, $^1J_{FC}$ = 272, Ar^F), 121.7 (d, $^3J_{PC}$ = 8, py), 121.5 (d, $^3J_{PC}$ = 8, py), 118.0 (sept, $^3J_{FC}$ = 4, Ar^F), 116.9 (s, C≡C*t*Bu), 105.3 (dd, $^2J_{PC}$ = 8, $^2J_{PC}$ = 5, IrCCH*t*Bu), 95.7 (app t, $^2J_{PC}$ = 10, IrCHCH*t*Bu), 60.1 (s, C≡C*t*Bu), 46.0 (d, $^1J_{PC}$ = 25, pyCH$_2$), 40.8 (d, $^1J_{PC}$ = 30, pyCH$_2$), 37.3 (s, CHCH*t*Bu{C}), 37.1 (s, CCH*t*Bu{C}), 36.6 (dd, $^1J_{PC}$ = 21, $^3J_{PC}$ = 4, P*t*Bu{C}), 34.6 (dd, $^1J_{PC}$ = 21, $^3J_{PC}$ = 6, P*t*Bu{C}), 33.3 (d, $^2J_{PC}$ = 15, CH$_2$), 32.2 (s, CH$_2$), 31.8 (s, C≡C*t*Bu{C}), 31.4 (s, CH$_2$), 31.28 (s, *t*Bu{CH$_3$}), 31.26 (s, *t*Bu{CH$_3$}), 31.1 (s, CH$_2$), 30.5 (s, CH$_2$), 30.3 (s, CH$_2$), 30.2 (s, CH$_2$), 29.7 (s, CHCH*t*Bu{CH$_3$}), 28.8 (br, CH$_2$), 28.20 (d, $^2J_{PC}$ = 4, CH$_2$), 28.17 (s, CH$_2$), 27.1 (d, $^2J_{PC}$ = 3, 2 × P*t*Bu{CH$_3$}), 26.6 (s, CH$_2$), 24.9 (s, CH$_2$), 21.9 (dd, $^1J_{PC}$ = 30, $^3J_{PC}$ = 2, PCH$_2$), 19.5 (dd, $^1J_{PC}$ = 19, $^3J_{PC}$ = 3, PCH$_2$).

^{31}P{^{1}H} NMR (162 MHz, CD_2Cl_2): δ 25.5 (d, $^2J_{PP}$ = 364, 1P), 16.8 (d, $^2J_{PP}$ = 364, 1P).

^{31}P{^{1}H} NMR (121 MHz, DFB): δ 25.0 (d, $^2J_{PP}$ = 364, 1P), 16.3 (d, $^2J_{PP}$ = 364, 1P).

HR ESI-MS (positive ion, 4 kV): 916.5623 ([*M*]$^+$, calcd 916.5628) *m*/*z*.

Anal. calcd for $C_{79}H_{95}BF_{24}IrNP_2$ (1779.57 g mol^{-1}): C, 53.35; H, 5.38; N, 0.79. Found: C, 53.26; H, 5.09; N, 0.77.

4.11 NMR scale reaction of 1 with *Z*-*t*BuC≡CCHCH*t*Bu

A solution of **1** (16.1, 9.8 μmol) in DFB (0.5 mL) within a J. Young valve NMR tube was treated with *Z*-*t*BuC≡CCHCH*t*Bu (4.6 mg, 28.0 μmol) and then heated at 50 °C for 1 h. No reaction was apparent upon analysis by NMR spectroscopy.

4.12 Crystallography

Data were collected on a Rigaku Oxford Diffraction SuperNova AtlasS2 CCD diffractometer using graphite monochromated Mo Kα (λ = 0.71073 Å) or CuKα (λ = 1.54184 Å) radiation and an Oxford Cryosystems N-HeliX low temperature device [150(2) K]. Data were collected and reduced using CrysAlisPro and refined using SHELXL,[39] through the Olex2 interface.[40] Full details about the collection, solution, and refinement are documented in CIF format, which have been deposited with the Cambridge Crystallographic Data Centre under CCDC 2051203 (**1**), 2051204 (**2**), 2051205 (**7**), 2051206 (**10**), 2051207 ([Rh(PNP-14)(η^2-norbornene)][BAr$^F{}_4$]).†

Conflicts of interest

There are no conflicts to declare.

Acknowledgements

We thank the European Research Council (ERC, grant agreement 637313) and Royal Society (UF100592, UF150675, A.B.C.) for financial support. High-resolution mass-spectrometry data were collected using instruments purchased through support from Advantage West Midlands and the European Regional Development Fund. Crystallographic data were collected using an instrument that received funding from the ERC under the European Union's Horizon 2020 research and innovation programme (grant agreement no. 637313).

References

1 (*a*) *Pincer Compounds: Chemistry and Applications*, ed. D. Morales-Morales, Elsevier, 2018, vol. 1; (*b*) R. E. Andrew, L. González-Sebastián and A. B. Chaplin, *Dalton Trans.*, 2016, **45**, 1299–1305; (*c*) *The Privileged Pincer-Metal Platform: Coordination Chemistry & Applications*, ed. G. van Koten and R. A. Gossage, Topics in Organometallic Chemistry, Springer, 2016, vol. 45; (*d*) J. R. Khusnutdinova and D. Milstein, *Angew. Chem., Int. Ed.*, 2015, **54**, 12236–12273; (*e*) *Pincer and Pincer–Type Complexes: Applications in Organic Synthesis and Catalysis*, ed. K. J. Szabó and O. F. Wendt, Wiley-VCH, 2014; (*f*) *Organometallic Pincer Chemistry*, ed. G. van Koten and D. Milstein, Topics in Organometallic Chemistry, Springer, 2013, vol. 40; (*g*) M. E. van der Boom and D. Milstein, *Chem. Rev.*, 2003, **103**, 1759–1792; (*h*) M. Albrecht and G. van Koten, *Angew. Chem., Int. Ed.*, 2001, **40**, 3750–3781.

2 E. Peris and R. H. Crabtree, *Chem. Soc. Rev.*, 2018, **47**, 1959–1968.

3 (*a*) M. D. Walter, P. S. White, C. K. Schauer and M. Brookhart, *J. Am. Chem. Soc.*, 2013, **135**, 15933–15947; (*b*) W. H. Bernskoetter, C. K. Schauer, K. I. Goldberg and M. Brookhart, *Science*, 2009, **326**, 553–556.

4 (*a*) A. Kumar, T. M. Bhatti and A. S. Goldman, *Chem. Rev.*, 2017, **117**, 12357–12384; (*b*) W. Yao, Y. Zhang, X. Jia and Z. Huang, *Angew. Chem., Int. Ed.*, 2014, **53**, 1390–1394; (*c*) J. Choi, A. H. R. MacArthur, M. Brookhart and A. S. Goldman, *Chem. Rev.*, 2011, **111**, 1761–1779; (*d*) A. S. Goldman, A. H. Roy, Z. Huang, R. Ahuja, W. Schinski and M. Brookhart, *Science*, 2006, **312**, 257–261; (*e*) M. Gupta, C. Hagen, R. J. Flesher, W. C. Kaska and C. M. Jensen, *Chem. Commun.*, 1996, 2083–2084.

5 (*a*) J. A. Labinger and J. E. Bercaw, *Nature*, 2002, **417**, 507–514; (*b*) A. E. Shilov and G. B. Shul'pin, *Chem. Rev.*, 1997, **97**, 2879–2932; (*c*) A. A. Bengali, R. H. Schultz, C. B. Moore and R. G. Bergman, *J. Am. Chem. Soc.*, 1994, **116**, 9585–9589; (*d*) J. K. Hoyano and W. A. G. Graham, *J. Am. Chem. Soc.*, 1982, **104**, 3723–3725; (*e*) A. H. Janowicz and R. G. Bergman, *J. Am. Chem. Soc.*, 1982, **104**, 352–354.

6 T. M. Hood, B. Leforestier, M. R. Gyton and A. B. Chaplin, *Inorg. Chem.*, 2019, **58**, 7593–7601.

7 A. J. Holmes, P. J. Rayner, M. J. Cowley, G. G. R. Green, A. C. Whitwood and S. B. Duckett, *Dalton Trans.*, 2015, **44**, 1077–1083.

8 (*a*) M. Findlater, K. M. Schultz, W. H. Bernskoetter, A. Cartwright-Sykes, D. M. Heinekey and M. Brookhart, *Inorg. Chem.*, 2012, **51**, 4672–4467; (*b*) A. B. Chaplin and A. S. Weller, *Organometallics*, 2011, **30**, 4466–4469.

9 W. H. Bernskoetter, S. K. Hanson, S. K. Buzak, Z. Davis, P. S. White, R. Swartz, K. I. Goldberg and M. Brookhart, *J. Am. Chem. Soc.*, 2009, **131**, 8603–8613.

10 D. Hermann, M. Gandelman, H. Rozenberg, L. J. W. Shimon and D. Milstein, *Organometallics*, 2002, **21**, 812–818.

11 M. R. Gyton, B. Leforestier and A. B. Chaplin, *Organometallics*, 2018, **37**, 3963–3971.

12 (*a*) C. M. Storey, M. R. Gyton, R. E. Andrew and A. B. Chaplin, *Chem. – Eur. J.*, 2020, **26**, 14715–17723; (*b*) C. M. Storey, A. Kalpokas, M. R. Gyton, T. Krämer and A. B. Chaplin, *Chem. Sci.*, 2020, **11**, 2051–2057; (*c*) C. M. Storey, M. R. Gyton, R. E. Andrew and A. B. Chaplin, *Angew. Chem., Int. Ed.*, 2018, **57**, 12003–12006.

13 (*a*) R. E. Andrew, C. M. Storey and A. B. Chaplin, *Dalton Trans.*, 2016, **45**, 8937–8944; (*b*) R. E. Andrew, D. W. Ferdani, C. A. Ohlin and A. B. Chaplin, *Organometallics*, 2015, **34**, 913–917; (*c*) R. E. Andrew and A. B. Chaplin, *Inorg. Chem.*, 2015, **54**, 312–322; (*d*) R. E. Andrew and A. B. Chaplin, *Dalton Trans.*, 2014, **43**, 1413–1423.

14 T. M. Hood, M. R. Gyton and A. B. Chaplin, *Dalton Trans.*, 2020, **49**, 2077–2086.

15 T. M. Hood and A. B. Chaplin, *Dalton Trans.*, 2020, **49**, 16649–16652.

16 (*a*) B. Leforestier, M. R. Gyton and A. B. Chaplin, *Angew. Chem., Int. Ed.*, 2020, **59**, 23500–23504; (*b*) B. Leforestier, M. R. Gyton and A. B. Chaplin, *Dalton Trans.*, 2020, **49**, 2087–2101.

17 G. E. M. Crisenza, N. G. McCreanor and J. F. Bower, *J. Am. Chem. Soc.*, 2014, **136**, 10258–10261.

18 Z. Lu, C.-H. Jun, S. R. de Gala, M. P. Sigalas, O. Eisenstein and R. H. Crabtree, *Organometallics*, 1995, **14**, 1168–1175.

19 For structurally related examples see: (*a*) P. Hermosilla, P. López, P. Garcia-Orduna, F. J. Lahoz, V. Polo and M. A. Casado, *Organometallics*, 2018, **37**, 2618–2629; (*b*) N. Grüger, H. Wadepohl and L. H. Gade, *Eur. J. Inorg. Chem.*, 2013, **2013**, 5358–5365; (*c*) P. Sánchez, M. Hernández-Juárez, E. Álvarez, M. Paneque, N. Rendón and A. Suárez, *Dalton Trans.*, 2016, **45**, 16997–17009; (*d*) J. J. Adams, N. Arulsamy and D. M. Roddick, *Organometallics*, 2011, **30**, 697–711; (*e*) M. Yamashita, Y. Moroe, T. Yano and K. Nozaki, *Inorg. Chim. Acta*, 2011, **369**, 15–18; (*f*) R. Sablong and J. A. Osborn, *Tetrahedron Lett.*, 1996, **37**, 4937–4940.

20 Generation of $[\{Rh(PNP\text{-}14)\}_2(\mu_2\text{–}\eta^2\text{:}\eta^2\text{-COD})]^{2+}$ under equilibrium is also implied in this case, as this dication was the species ultimately obtained upon crystallisation (see ref. 15). Mononuclear formulation in solution is, however, substantiated by synthesis of $[Rh(PNP\text{-}14)(\eta^2\text{-norbornene})][BAr^F{}_4]$ ($\delta_{^{31}P}$ 71.2, 55.9; $^2J_{PP}$ = 244 Hz). Details, including solid-state structure, are provided in the ESI.†

21 P. S. Pregosin, *NMR in Organometallic Chemistry*, Wiley-VCH, 2012, pp. 258–264.

22 (*a*) A. A. Danopoulos, D. Pugh and J. A. Wright, *Angew. Chem., Int. Ed.*, 2008, **47**, 9765–9767; (*b*) P. Paredes, J. Díez and M. P. Gamasa, *Organometallics*, 2008, **27**, 2597–2607; (*c*) J. Díez, M. P. Gamasa, J. Gimeno and P. Paredes, *Organometallics*, 2005, **24**, 1799–1802.

23 Mono-ethylene complexes have instead been reported, see: ref. 8*a* and 25*f*.

24 Reaction of **7** with dihydrogen (1 atm) in DFB regenerates **4** in quantitative spectroscopic yield, within 16 h at 80 °C.

25 (*a*) S. Gu, R. J. Nielsen, K. H. Taylor, G. C. Fortman, J. Chen, D. A. Dickie, W. A. Goddard III and T. B. Gunnoe, *Organometallics*, 2020, **39**, 1917–1933; (*b*) M. Rimoldi, A. Nakamura, N. A. Vermeulen, J. J. Henkelis, A. K. Blackburn, J. T. Hupp, J. F. Stoddart and O. K. Farha, *Chem. Sci.*, 2016, **7**, 4980–4984; (*c*) S. Kundu, J. Choi, D. Y. Wang, Y. Choliy, T. J. Emge, K. Krogh-Jespersen and A. S. Goldman, *J. Am. Chem. Soc.*, 2013, **135**, 5127–5143; (*d*) K. S. Lokare, R. J. Nielsen, M. Yousufuddin, W. A. Goddard III and R. A. Periana, *Dalton Trans.*, 2011, **40**, 9094; (*e*) A. V. Polukeev, S. A. Kuklin, P. V. Petrovskii, A. S. Peregudov, F. M. Dolgushin, M. G. Ezernitskaya and A. A. Koridze, *Russ. Chem. Bull.*, 2010, **59**, 745–749; (*f*) T. Yano, Y. Moroe, M. Yamashita and K. Nozaki, *Chem. Lett.*, 2008, **37**, 1300–1301; (*g*) F. Novak, B. Speiser, H. A. Y. Mohammad and H. A. Mayer, *Electrochim. Acta*, 2004, **49**, 3841–3853; (*h*) H. A. Y. Mohammad, J. C. Grimm, K. Eichele, H.-G. Mack, B. Speiser, F. Novak, M. G. Quintanilla, W. C. Kaska and H. A. Mayer, *Organometallics*, 2002, **21**, 5775–5784; (*i*) S. Nemeh, C. Jensen, E. Binamira-Soriaga and W. C. Kaska, *Organometallics*, 1983, **2**, 1442–1447.

26 S. Khorasani, M. A. Fernandes and C. B. Perry, *Cryst. Growth Des.*, 2012, **12**, 5908–5916.

27 G. L. Parker, S. Lau, B. Leforestier and A. B. Chaplin, *Eur. J. Inorg. Chem.*, 2019, **2019**, 3791–3798.

28 (*a*) L. Maser, C. Schneider, L. Vondung, L. Alig and R. Langer, *J. Am. Chem. Soc.*, 2019, **141**, 7596–7604; (*b*) J. J. Davidson, J. C. DeMott, C. Douvris, C. M. Fafard, N. Bhuvanesh, C.-H. Chen, D. E. Herbert, C.-I. Lee, B. J. McCulloch, B. M. Foxman and O. V. Ozerov, *Inorg. Chem.*, 2015, **54**, 2916–2935.

29 S. M. Chapp and N. D. Schley, *Inorg. Chem.*, 2020, **59**, 7143–7149.

30 R. Ghosh, X. Zhang, P. Achord, T. J. Emge, K. Krogh-Jespersen and A. S. Goldman, *J. Am. Chem. Soc.*, 2007, **129**, 853–866.

31 For examples of iridium catalysed terminal alkyne coupling reactions see: (*a*) M. Ez-Zoubir, F. Le Boucher d'Herouville, J. A. Brown, V. Ratovelomanana-Vidal and V. Michelet, *Chem. Commun.*, 2010, **46**, 6332–6334; (*b*) K. Ogata and A. Toyota, *J. Organomet. Chem.*, 2007, **692**, 4139–4146; (*c*) T. Ohmura, S.-I. Yorozuya, Y. Yamamoto and N. Miyaura, *Organometallics*, 2000, **19**, 365–367; (*d*) C.-H. Jun, Z. Lu and R. H. Crabtree, *Tetrahedron Lett.*, 1992, **33**, 7119–7120.

32 J. Alós, T. Bolaño, M. A. Esteruelas, M. Oliván, E. Oñate and M. Valencia, *Inorg. Chem.*, 2013, **52**, 6199–6213.

33 The bis(ethylene) complex **6** is also an effective precatalyst for this reaction (complete conversion within 6 h using 1 mol% loading). Full details are provided in the ESI.†

34 For a crystallographically characterised iridium η^1-enynyl complexes see: (*a*) J. S. Merola, T. L. Husebo and K. E. Matthews, *Organometallics*, 2012, **31**, 3920–3929; (*b*) K. Ilg and H. Werner, *Chem. – Eur. J.*, 2002, **8**, 2812–2820; (*c*) T. X. Le and J. S. Merola, *Organometallics*, 1993, **12**, 3798–3799.

35 For reviews see: (*a*) O. N. Temkin, *Kinet. Catal.*, 2020, **60**, 689–732; (*b*) Q. Liang, K. Hayashi and D. Song, *ACS Catal.*, 2020, **10**, 4895–4905; (*c*) B. M. Trost and J. T. Masters, *Chem. Soc. Rev.*, 2016, **45**, 2212–2238.

36 For recent or notable examples see: (*a*) N. Gorgas, B. Stöger, L. F. Veiros and K. Kirchner, *ACS Catal.*, 2018, **8**, 7973–7982; (*b*) O. Rivada-Wheelaghan, S. Chakraborty, L. J. W. Shimon, Y. Ben-David and D. Milstein, *Angew. Chem., Int. Ed.*, 2016, **55**, 6942–6945; (*c*) J. Alós, T. Bolaño, M. A. Esteruelas, M. Oliván, E. Oñate and M. Valencia, *Inorg. Chem.*, 2014, **53**, 1195–1209; (*d*) H. Katayama, H. Yari, M. Tanaka and F. Ozawa, *Chem. Commun.*, 2005, 4336–4338; (*e*) C. Bianchini, M. Peruzzini, F. Zanobini, P. Frediani and A. Albinati, *J. Am. Chem. Soc.*, 1991, **113**, 5453–5454; see also ref. 32.

37 S. D. Pike, M. R. Crimmin and A. B. Chaplin, *Chem. Commun.*, 2017, **53**, 3615–3633.

38 (*a*) A. J. Martínez-Martínez and A. S. Weller, *Dalton Trans.*, 2019, **48**, 3551–3554; (*b*) W. E. Buschmann, J. S. Miller, K. Bowman-James and C. N. Miller, *Inorg. Synth.*, 2002, **33**, 83–91.

39 G. M. Sheldrick, *Acta Crystallogr., Sect. C: Struct. Chem.*, 2015, **71**, 3–8.

40 O. V. Dolomanov, L. J. Bourhis, R. J. Gildea, J. A. K. Howard and H. Puschmann, *J. Appl. Crystallogr.*, 2009, **42**, 339–341.